Influence of Coexisting Chronic Kidney Disease and Left Ventricular Hypertrophy on Changes in FGF23 and the Renin-Angiotensin-Aldosterone-System

Kohei Okamoto
Kobe University Graduate School of Medicine
Hideki Fujii (fhideki@med.kobe-u.ac.jp)
Kobe University Graduate School of Medicine
Shunsuke Goto
Kobe University Graduate School of Medicine
Kentaro Watanabe
Kobe University Graduate School of Medicine
Keiji Kono
Kobe University Graduate School of Medicine
Shinichi Nishi
Kobe University Graduate School of Medicine

Research Article

Keywords: aldosterone, chronic kidney disease, fibroblast growth factor 23, left ventricular hypertrophy, renin-angiotensin-aldosterone system

Posted Date: June 24th, 2021

DOI: https://doi.org/10.21203/rs.3.rs-634094/v1

Abstract

Serum fibroblast growth factor 23 (FGF23) levels and the renin-angiotensin-aldosterone system (RAAS) are elevated in chronic kidney disease (CKD) patients, and their association with left ventricular hypertrophy (LVH) has been reported. However, whether the FGF23 elevation is the cause or result of LVH remains unclear. At 10 weeks, male C57BL/6J mice were divided into four groups: Sham, CKD (5/6 nephrectomy), LVH (transaortic constriction), and CKD/LVH group. At 16 weeks, the mice were sacrificed, and blood and urine, cardiac expressions of FGF23 and RAAS-related factors, and cardiac histological analyses were performed. Heart weight, serum FGF23 levels, and cardiac expression of FGF23 and RAAS-related factors, except for angiotensin-converting enzyme 2, more increased in the CKD/LVH group compared to the other groups. A significant correlation between LVH and cardiac expressions of FGF23 and RAAS-related factors was observed. Furthermore, there was a significantly close correlation of the cardiac expression of FGF23 with LVH and RAAS-related factors. The coexisting CKD and LVH increased serum and cardiac FGF23 and RAAS-related factors, and there was a significant correlation between them. A close correlation of cardiac, but not serum FGF23, with LVH and RAAS suggested that local FGF23 may be associated with LVH and the RAAS activation.

Introduction

Fibroblast growth factor 23 (FGF23) is a crucial phosphaturic hormone, and its serum level increases as kidney function declines [1]. FGF23 is mainly produced in the bone and interacts with the FGF23 receptor (FGFR) in the presence of klotho in the kidney proximal tubule. In this way, phosphorus diuresis is promoted in the kidney. However, FGF23 also has many other actions [2]. One of them is a potential action on left ventricular hypertrophy (LVH) progression [3, 4]. Although previous experimental studies have reported that considerably high levels of serum FGF23 could induce LVH via FGFR4-mediated calcineurin-NFAT pathway activation even in the absence of αKlotho [4], clinical studies have shown a significant correlation between serum FGF23 levels and LVH even in patients with a mild or moderate elevation of serum FGF23 levels [3]. In addition, it has also been reported that the FGF23 gene deletion mice underwent transverse aortic constriction (TAC) reveal LVH [5]. Although patients with tumor-induced osteomalacia have remarkably high serum FGF23 levels and FGF23-related hypophosphatemia, serum FGF23 levels are not associated with LVH [6]. Thus, whether LVH progresses by an increase in FGF23 or whether the occurrence of LVH increases FGF23 are still unclear, and we do not yet have a consensus on which is the primary cause.

Recent studies have demonstrated a close correlation between FGF23 and the renin-angiotensin-aldosterone system (RAAS) [7]. The RAAS is an important control system for blood pressure and causes LVH [8]. Therefore, we focused on the RAAS as a common factor for an increase in FGF23 and the exacerbation of LVH.

This study aimed to verify FGF23 and RAAS changes and their correlation using a chronic kidney disease (CKD) model, a model for pressure overload-induced cardiac hypertrophy, and a combined model.

Results

Animal characteristics and biochemical measurements

The characteristics and biochemical data at 16 weeks in the sham, CKD, LVH, and CKD/LVH groups are shown in Table 1. BP was significantly elevated in the CKD and CKD/LVH groups. Serum Cr levels, phosphate levels, and uAlb excretion significantly increased in the CKD and CKD/LVH groups compared to the sham group. Serum calcium levels were comparable among the four groups. Although uAlb excretion was comparable between the sham and LVH groups, and serum Cr levels were slightly elevated in the LVH group compared to the sham group. Serum iPTH levels were elevated in the CKD and LVH groups compared to the sham group, although there was no statistically significant difference; however, they were significantly higher in the CKD/LVH group. Serum 25D levels were similar among all the study groups, and serum 1,25D levels decreased by CKD induction. Urinary 8-OHdG levels were significantly higher in the CKD and CKD/LVH groups than in the sham group. As shown in Fig. 1, although serum iFGF23 levels were significantly elevated in the CKD, LVH, and CKD/LVH groups compared to the sham group, there was no statistically significant difference among the three groups, except for the sham group. In contrast, serum aldosterone levels increased by CKD and LVH induction, and they were additionally increased by coexisting CKD and LVH.

Table 1
Animal characteristics at 16 weeks

	Sham (N = 6)	CKD (N = 6)	LVH (N = 6)	CKD/LVH (N = 6)
Body weight (g)	29. 5 ± 0.7	25.1 ± 0.8#	28.7 ± 0.6*	25.7 ± 1.0#, ▯
SBP (mmHg)	86.2 ± 0.6	97.6 ± 2.0#	87.2 ± 1.8	107.2 ± 4.0#, ▯
HR (/min)	516.3 ± 12.3	493.1 ± 12.2	490.7 ± 15.4	472.8 ± 14.7
Cr (mg/dL)	0.14 ± 0.02	0.44 ± 0.03#	0.23 ± 0.02*	0.47 ± 0.09#, ▯
Ca(mg/dL)	9.87 ± 0.30	9.83 ± 0.80	10.03 ± 0.76	9.02 ± 0.81
P (mg/dL)	8.1 ± 0.6	9.7 ± 0.4#	8.8 ± 0.3	10.3 ± 0.3#
iPTH (pg/mL)	29.0 ± 11.6	77.6 ± 16.2	50.6 ± 7.0	111.6 ± 39.1#
25(OH)D (pg/mL)	61.7 ± 2.3	61.8 ± 3.5	59.7 ± 3.2	63.3 ± 4.0
1, 25$(OH)_2$D (pg/mL)	227.0 ± 18.9	184.8 ± 10.4	222.2 ± 24.6	178.0 ± 9.9
uAGT (ng/mgCr)	3.32 ± 0.85	3.36 ± 0.94	7.13 ± 2.55#, *	9.62 ± 2.10#, *
uAlb (μg/mgCr)	144.6 ± 9.5	1156.3 ± 221.2#	156.1 ± 5.7*	1356.8 ± 145.6#, ▯
u8-OHdG (ng/mgCr)	53.9 ± 1.8	99.4 ± 16.1#	82.8 ± 8.3	101.3 ± 9.2#

#: vs Sham, $P < 0.05$, *: vs CKD, $P < 0.05$, ▯: vs LVH, $P < 0.05$.

CKD, chronic kidney disease; LVH, left ventricular hypertrophy; SBP, systolic blood pressure; HR, heart rate; Cr, creatinine; Ca, calcium; P, phosphate; iPTH, intact parathyroid hormone; uAGT, urinary angiotensinogen; uAlb, urinary albumin; u8-OHdG, urinary 8-hydroxy-2'-deoxyguanosine.

Cardiac Parameters After Induction Of Ckd And Lvh

Cardiac parameters evaluated using echocardiography and heart weight are shown in Table 2. As for the LV dimension, LV end-diastolic diameter and LV end-systolic diameter were smaller in the CKD/LVH group compared to other groups. Both anterior and posterior wall of the LV remarkably thickened in the LVH and CKD/LVH group. Systolic function revealed as ejection fraction (EF) was significantly reduced in the LVH and CKD/LVH groups compared to the sham and CKD groups. The relative heart weight (heart weight/body weight) was significantly higher in the order of the CKD/LVH, LVH, CKD, and sham groups.

Table 2
Animal characteristics at 16 weeks

	Sham (N = 6)	CKD (N = 6)	LVH (N = 6)	CKD/LVH (N = 6)
LVDd (mm)	3.77 ± 0.76	3.45 ± 0.76	3.47 ± 0.29	3.15 ± 0.08
LVDs (mm)	2.78 ± 0.06	2.67 ± 0.06	2.75 ± 0.22	2.55 ± 0.07#, *
LVAW (mm)	0.75 ± 0.02	0.80 ± 0.04	1.23 ± 0.04#, *	1.30 ± 0.04#, *
LVPW (mm)	0.71 ± 0.03	0.75 ± 0.04	1.18 ± 0.05#, *	1.20 ± 0.04#, *
FS (%)	25.8 ± 0.4	23.0 ± 0.2#	20.9 ± 0.3#, *	19.3 ± 0.8#, *
EF (%)	57.7 ± 0.6	52.9 ± 0.4	49.1 ± 0.5#, *	46.0 ± 1.7#, *
Heart weight (mg)	131.3 ± 3.3	116.2 ± 2.3	181.6 ± 5.2#, *	178.2 ± 8.5#, *
Relative heart weight (mg/g)	4.45 ± 0.07	4.64 ± 0.08	6.33 ± 0.16#, *	6.96 ± 0.36#, *

#: vs Sham, $P < 0.05$, *: vs CKD, $P < 0.05$, ▯: vs LVH, $P < 0.05$.

CKD, chronic kidney disease; LVH, left ventricular hypertrophy; LVDd, left ventricular diastolic diameter; LVDs, left ventricular systolic diameter; LVAW, left ventricular anterior wall; LVPW, left ventricular posterior wall; FS, fractional shortening; EF, ejection fraction.

Coexisting CKD and LVH deteriorate cardiac hypertrophy and cardiac interstitial fibrosis

As shown in Fig. 2, cardiomyocyte width and area increased by LVH and CKD induction. Coexisting LVH and CKD are related to the further development of cardiac hypertrophy. Cardiac fibrosis was also significantly deteriorated in the CKD and CKD/LVH groups (Fig. 3).

Cardiac expressions of FGF23, RAAS-related factors, and cardiac hypertrophy-related factors induced by CKD and LVH

Cardiac FGF23 mRNA expression significantly increased in the CKD and LVH groups and further increased in the CKD/LVH group. Similarly, cardiac angiotensinogen (AGT) mRNA expression significantly increased in the LVH group and further increased in the CKD/LVH group. The cardiac AT1R and ACE mRNA expression significantly increased in the CKD/LVH group. In contrast, cardiac ACE2 mRNA expression significantly decreased in the LVH group and further decreased in the CKD/LVH group (Fig. 4).

In addition, the immunohistochemical analysis also showed that expression of FGF23 and ACE significantly increased in the CKD/LVH group. Corresponding with RT-PCR results, angiotensin II significantly increased in the LVH and CKD/LVH groups, and the expression of ACE2 significantly decreased in the LVH and CKD/LVH groups (Fig. 5).

As for bone FGF23 mRNA expression, it slightly increased in the LVH group compared to the sham group and remarkably increased by CKD induction (Fig. 6).

mRNA expression of factors related to cardiac hypertrophy and fibrosis increased by CKD and LVH induction

The cardiac β-MHC, ANP, BNP, Col1a2, and Col3a1 mRNA expressions significantly increased, whereas cardiac α-MHC mRNA expression significantly decreased in the CKD/LVH group. In the LVH group, cardiac β-MHC mRNA expression also significantly increased, and cardiac α-MHC mRNA expression significantly decreased compared to the sham group (Fig. 7).

Correlation between FGF23, RAAS-related factors and cardiac hypertrophy and fibrosis

Serum FGF23 levels, cardiac FGF23 expressions (mRNA and immunohistochemical staining), and RAAS-related factors were related to cardiac hypertrophy parameters (width and size of cardiomyocyte) and mRNA expressions of cardiac hypertrophy and fibrosis-related factors. However, the correlation of serum FGF23 levels with them was weaker than that of cardiac FGF23 expressions and RAAS-related factors (Table 3). Although cardiac FGF23 expressions were significantly correlated with all the RAAS-related factors, serum FGF23 was significantly correlated with only cardiac mRNA expression of AT1R and AGT and the immunohistochemical expressions of angiotensin II and ACE (Table 4). Thus, the correlation of cardiac FGF23 expression with RAAS-related factors was closer than that of serum FGF23 with RAAS-related factors.

Table 3
Correlation of each FGF23 and RAAS data with cardiac parameters

	HW	rHW	Width	Area	Fibrosis	LVAW	LVPW	FS	EF	cANP	cBNP	cα-MHC	cβ-MHC	c(
iFGF23	.212	.517**	.617**	.518**	.698**	.449*	.394	− .639**	− .645**	.329	.299	− .181	.583**	.4
cFGF23	.536**	.708**	.641**	.717**	.807**	.726**	.707**	− .816**	− .805**	.399	.436*	− .512*	.846**	.7
imFGF23	.505*	.766**	.649**	.815**	.890**	.728**	.709**	− .820**	− .814**	.403	.538**	− .569**	.838**	.6
Ald	.251	.641**	.666**	.495*	.616**	.564**	.566**	− .629**	− .625**	.241	.239	− .241	.527**	.5
cAT1R	.624**	.765**	.679**	.830**	.768**	.702**	.644**	− .858**	− .863**	.369	.427*	− .651**	.742**	.5
cAGT	.537**	.674**	.730**	.678**	.662**	.779**	.700**	− .692**	− .691**	.490*	.352	− .703**	.742**	.4
cACE	.823**	.784**	.600**	.683**	.628**	.735**	.705**	− .717**	− .714**	.441*	.448*	− .773**	.738**	.4
cACE2	− .690**	− .778**	− .613**	− .701**	− .622**	− .752**	− .702**	.714**	.704**	− .528**	− .311	.803**	− .699**	−
uAGT	.485*	.572**	.528**	.557**	.557**	.744**	.694**	− .624**	− .612**	.116	.213	− .539**	.683**	.5
imAng II	.448*	.656**	.651**	.562**	.637**	.665**	.613**	− .672**	− .676**	.301	.283	− .561**	.714**	.3
imACE	.700**	.836**	.779**	.853**	.824**	.837**	.821**	− .884**	− .881**	.462*	.561**	− .695**	.834**	.6
imACE2	− .690**	− .776**	− .664**	− .586**	− .643**	− .834**	− .794**	.706**	.705**	− .489*	− .476*	.719**	− .786**	−

*: $P < 0.05$, **: $P < 0.01$.

HF, heart weight; rHF, relative heart weight; LVAW, left ventricular anterior wall; LVPW, left ventricular posterior wall; FS, fractional shortening; EF, ejection fracti atrial natriuresis peptide; cBNP, cardiac brain natriuresis peptide; cα-MHC, cardiac α-myosin heavy chain; cβ-MHC, cardiac β-myosin heavy chain; cCol1a2, car I α2; cCol3a1, cardiac collagen type III α1; iFGF23, intact fibroblast growth factor 23; cFGF23, cardiac fibroblast growth factor 23; imFGF23, immunohistocher of cardiac fibroblast growth factor 23; Ald, aldosterone; cAT1R, cardiac angiotensin II type 1 receptor; cAGT, cardiac angiotensinogen; cACE, cardiac angiotens enzyme; cACE2, cardiac angiotensin-converting enzyme 2; uAGT, urinary angiotensinogen; imAng II, immunohistochemical expression of cardiac angiotensin immunohistochemical expression of cardiac angiotensin-converting enzyme; imACE2, immunohistochemical expression of cardiac angiotensin-converting e

Table 4
Correlation of each FGF23 data with RAAS-related factors

	Ald	cAT1R	cAGT	cACE	cACE2	uAGT	imAng II	imACE	imACE2
iFGF23	.388	.665**	.556**	.285	− .269	.164	.511*	.518**	− .297
cFGF23	.567**	.780**	.722**	.663**	− .689**	.626**	.713**	.785**	− .666**
imFGF23	.554**	.820**	.762**	.664**	− .623**	.554**	.729**	.862**	− .705**

Ald, aldosterone; cAT1R, cardiac angiotensin II type 1 receptor; cAGT, cardiac angiotensinogen; cACE, cardiac angiotensin-converting enzyme; cACE2, cardiac angiotensin-converting enzyme 2; uAGT, urinary angiotensinogen; imAng II, immunohistochemical expression of cardiac angiotensin II; imACE, immunohistochemical expression of cardiac angiotensin-converting enzyme; imACE2, immunohistochemical expression of cardiac angiotensin-converting enzyme 2; iFGF23, intact fibroblast growth factor 23; cFGF23, cardiac fibroblast growth factor 23; imFGF23, immunohistochemical expression of cardiac fibroblast growth factor 23.

Discussion

We demonstrated that 1) CKD deteriorated LVH and cardiac fibrosis induced by TAC; 2) serum FG23 and aldosterone levels increased in the CKD and LVH groups, and further elevation of these levels was observed in the CKD/LVH group; 3) similarly, intracardiac FGF23, hypertrophy-related factors, fibrosis-related factors, and RAAS-related factors increased in the LVH and CKD groups and dramatically increased in the CKD/LVH group; 4) among the RAAS-related factors, only ACE2 decreased by LVH, CKD, and CKD/LVH induction; 5) heart weight was significantly correlated with serum FGF23 and aldosterone levels and intracardiac expression of FGF23 and the RAAS-related factors.

It is well known that pressure overload and CKD induce LVH. The development of LVH in these conditions involves various pathophysiological mechanisms. In pressure overload-induced LVH, cardiomyocyte hypertrophy and interstitial fibrosis reportedly occur through the activated mitogen-activated protein kinase (MAPK) pathway [14], increase in oxidative stress [15], and the activation of RAAS [16]. The results of our study also showed an increase in urinary excretion of 8-OHdG, an elevation of serum aldosterone levels, and an increase in the expression of AT1R, AGT, and ACE in the heart. In CKD, not only these factors but also CKD-related factors are involved in the progression of LVH. Recent compelling evidences suggest that CKD and mineral bone disorder (CKD-MBD) is strongly linked to the progression of cardiovascular disease in these populations [17]. Among the CKD-related factors, phosphate, calcium, FGF23, PTH, Klotho, and 1, 25 $(OH)_2$ D were thought to play key roles. Many experimental and clinical studies have reported the correlation between FGF23 and LVH [18, 19]. It has been reported that the elevation of FGF23 directly causes myocardial hypertrophy even if klotho does not coexist with FGFR [4, 20]. Among FGFRs, FGFR4 is thought to have an important role in the progression of LVH through the activation of the calcineurin-NFAT pathway [4, 20]. However, the previous experimental study using cardiomyocyte-specific calcineurin A-transgenic mice showed that LVH induced an increase in myocardial and serum FGF23 [21]. In other words, this might mean that activation of the calcineurin-NFAT pathway could increase FGF23. Therefore, we performed an experimental study using a surgical model of CKD, LVH, and CKD/LVH to ascertain changes in RAAS and CKD-MBD parameters, including FGF23. Although serum and cardiac FGF23 increased in CKD as previously reported, these also increased even in LVH without CKD. In addition, further elevation of FGF23 was observed in CKD/LVH. However, as serum FGF23 levels in the CKD/LVH group were approximately 2-fold higher compared to those in the sham group, they did not seem to be enough to bind to FGFR without klotho.

On the other hand, serum aldosterone levels in the CKD group rose approximately 5-fold as high as those in the sham group, and intracardiac mRNA expression of RAAS-related factors also increased in the CKD/LVH group. In our previous study using hypertensive model rats, an increase in serum FGF23 levels was also trivial. In contrast, an increase in serum aldosterone levels was much greater in the hypertensive group than in the sham group [22]. Furthermore, serum FGF23 levels were not correlate with LVH in pediatric CKD patients with preserved kidney function and FGF23-related hypophosphatemic diseases [6, 23]. From these findings, it is speculated that the influence of RAAS on LVH is greater than that of FGF23.

To date, various studies have reported the interaction between RAAS and FGF23 [24–26]. An in vitro study using cardiomyocytes demonstrated that Ang II and aldosterone significantly upregulated FGF23 mRNA expression, suggesting that activation of the RAAS leads to the induction of FGF23 in cardiac myocytes [27]. In contrast, FGF23 also increased intracellular angiotensin II expression in cardiomyocytes [7]. Both RAAS and FGF23 are thought to be closely related to the pathophysiological mechanisms of the progression of LVH and cardiac fibrosis. Our previous study showed a significant relationship between serum FGF23 and aldosterone levels, and both were significantly correlated with heart weight [22]. Even in the present study, both RAAS-related factors and FGF23 increased in cardiac tissues in the CKD and LVH groups. The increase was manifest, particularly in the CKD/LVH group. Serum FGF23 levels, intracardiac FGF23 expression, serum aldosterone levels, and intracardiac RAAS-related factors expressions were significantly correlated with heart weight. Particularly, a significantly close correlation between intracardiac RAAS-related factors and FGF23 was observed. There is surely a close link between intracardiac RAAS and FGF23, and this interaction could play a key role in the progression of LVH.

We assessed the influence of LVH on CKD-MBD parameters. The increase in FGF23 decreases 1, 25 $(OH)_2$ D by reducing the expression of 1α-hydroxylase [28] and led to increased renin activity [29]. In addition, 1, 25 $(OH)_2$ D is also considered a crucial factor in the progression of LVH because cardiac-specific vitamin D receptor knock-out mice showed marked cardiac hypertrophy [30], and a vitamin D receptor activator could prevent the progression of LVH independently of RAAS [31]. The present study also showed that serum 1, 25 $(OH)_2$ D decreased in the CKD and CKD/LVH groups despite similar serum 25 (OH) D levels. ACE2 is an enzyme that can convert angiotensin I to angiotensin (1–9) and angiotensin II to angiotensin (1–7) [32, 33]. Angiotensin (1–9) and angiotensin (1–7) can lower BP by their vasodilative effect. Thus, they could prevent the LVH progression. ACE2-deficient mice developed cardiac dysfunction and LVH,

enhanced oxidative stress, and inflammatory cytokine expression [34–36]. Interestingly, intracardiac ACE2 expression dramatically decreased in the LVH and CKD + LVH groups, and ACE is supposed to be an important factor in the progression of LVH. It has been reported that FGF23 decreases ACE2 expression [37] and that plasma ACE2 activity is impaired in CKD patients [38]. Therefore, this mechanism might greatly contribute to the progression of LVH in CKD.

The most important limitation of this study is that we could not clarify the first occurrence regarding the relationship between RAAS and FGF23. From the degree of change in FGF23, FGF23 could not be a contributor to the progression of LVH. However, there is a possibility that FGF23 may induce LVH in a paracrine or autocrine manner, or both. FGF23 and RAAS enhance the expression of cardiac hypertrophy- and cardiac fibrosis-related factors via various pathways, such as the MAPK pathway, the TGF-β-Smad pathway, the NFκB pathway, and the NFAT-CnB pathway [14, 21, 39]. Unfortunately, our study could not adequately evaluate these pathways. As for intracardiac calcineurin B expression, there was no significant difference among the study groups. Moreover, we did not perform an interventional study with the FGFR blocker, ACE inhibitor, angiotensin receptor blocker, or aldosterone blocker. To resolve this issue, we need to plan a further study.

In conclusion, coexisting CKD and LVH further increased serum aldosterone and FGF23 levels and cardiac expression of FGF23 and RAAS-related factors. There was a significantly close correlation of not serum but cardiac FGF23 with LVH and RAAS, suggesting that local FGF23 may be associated with the activation of the RAAS and LVH.

Methods

Animals

Male C57BL/6J mice were obtained from SLC Japan Inc., Shizuoka, Japan. The mice were housed with food and water available ad libitum in light- and temperature-controlled environments. The mice were randomly divided into four groups at 10 weeks of age: sham-operated mice (sham, n = 6), induced-CKD mice (CKD, n = 6), induced-LVH mice (LVH, n = 6), and induced-CKD and induced-LVH mice (CKD/LVH, n = 6). At 10 weeks, TAC was performed for mice in the LVH and CKD/LVH groups. Briefly, the mice were anesthetized with isoflurane, and medetomidine, midazolam, and butorphanol were intraperitoneally administered. They were intubated with 22 G vascular catheters and then artificially ventilated (Small Animal Ventilator MK-V100, Muromachi Kikai). The thorax was opened, the aorta was exteriorized and a ligature was placed around the aorta as previously described [9]. The needle used for ligation was 27 G. At 11 weeks, a left 2/3 nephrectomy was performed, and one week later, a right nephrectomy was also performed for mice in the CKD and CKD/LVH groups. For mice in the sham group, sham operations were performed at 10, 11, and 12 weeks of age. Echocardiographic parameters were measured and 24-hour urine samples were collected from each mouse using a metabolic cage before the mice were sacrificed. At 16 weeks, these mice were sacrificed under anesthesia. Blood samples for serum measurements were collected from the right ventricle, and the hearts and bones were removed for RNA extraction and histomorphological analysis.

This study was carried out in strict accordance with the recommendations in the Guide for the Care and Use of Laboratory Animals of the National Institutes of Health. The protocol was approved by the Animal Experiment Facility Ethics Committee, Graduate School of Medicine, Kobe University (Permit Number: P160707-R2). All surgery was performed under anesthesia with 1.5 % isoflurane with intraperitoneal medetomidine, midazolam, and butorphanol premedication (0.15 mg/kg medetomidine, 2 mg/kg midazolam, and 2.5 mg/kg butorphanol. Efforts were made to minimize suffering by following the ARRIVE guidelines for reporting experiments involving animals [10, 11]. A randomized protocol was used in the experiments with a total of 24 mice.

Blood And Urine Measurement

Collected blood was centrifuged for 15 min at 3,000 rpm and stored at -80°C until analysis. Serum creatinine (Cr) levels were measured using a Fuji Dri-chem 3500 (FUJIFILM Japan, Tokyo, Japan). Serum phosphate, intact parathyroid hormone (iPTH), intact fibroblast growth factor 23 (iFGF23), and aldosterone levels were measured using ELISA (phosphate: FUJIFILM Japan, Tokyo, Japan; iPTH: Cloud-Clone Corp., Houston, Texas, USA; iFGF23: Kainos Laboratories, Inc., Tokyo, Japan; Aldosterone: Abcam, Cambridge, UK). Urinary excretion of albumin (uAlb), urinary Cr levels, urinary angiotensinogen (uAGT) levels, and 8-hydroxydeoxyguanosine (u8-OHdG) were also determined using ELISA (uAlb: FUJIFILM Wako Shibayagi Corporation, Gunma, Japan; u-Cr: FUJIFILM Wako Pure Chemicals Corporation, Osaka, Japan; uAGT: MyBioSource, San Diego, CA, USA; u8-OHdG: Japan Institute for Control of Aging, Shizuoka, Japan). Serum 25-hydroxyvitamin D (25D) and 1,25-dihydroxyvitamin D (1,25D) levels were measured using 25D125I radioimmunoassay kit (DIAsource ImmunoAssays S.A., Nivelles, Belgium) and a TFB 1,25D radioimmunoassay kit (Immunodiagnostic Systems Ltd., Boldon, UK), respectively.

Blood Pressure Measurements

Systolic blood pressure (BP) was measured using tail-cuff plethysmography (Model MK-2000; Muromachi Kikai Co. Ltd., Japan). The mice rested for 15min to reduce stress-induced BP elevation. The mean value was determined using multiple readings (at least 10). The BP evaluation was performed at the end of the study period.

Echocardiographic Measurements

The mice were mildly anesthetized with 1.0 % isoflurane. Echocardiography was performed using a commercially available echocardiographic system (F37; Hitachi Aloka Medical, Ltd, Tokyo, Japan). The wall thickness and ejection fraction (EF) were measured using a two-dimensional short-axis view of the left ventricle (LV) at the papillary muscle level. These studies were performed at 16 weeks.

Histological And Immunohistochemical Analyses

The hearts were removed, weighed, and fixed in 10 % formaldehyde. The paraffin block was made by immersing the samples in ethanol, xylene, and paraffin in the embedding device at room temperature. The paraffin blocks were cut into 2-μm sections and stained with hematoxylin-eosin for routine histology and

Sirius red for morphometric studies.

FGF23, angiotensin II, angiotensin converting enzyme (ACE), and angiotensin converting enzyme 2 (ACE2) expression in the heart were assessed with anti-FGF23 monoclonal antibodies (R&D Systems, Minneapolis, MN, USA), anti-angiotensin II monoclonal antibodies (Novus Biologicals, LLC, Littleton, Colorado, USA), anti-ACE monoclonal antibodies (Abcam, Cambridge, UK), and anti-ACE2 monoclonal antibodies (R&D Systems, Minneapolis, MN, USA). In brief, heart slices were preincubated with blocking agents and then incubated with the primary antibodies mentioned above for 60 min at room temperature (ACE, FGF23) and overnight at 4 ℃ (ACE2, angiotensin II). Biotinylated Anti-rat and Anti-goat IgG (Vector Laboratories, Burlingame, CA, USA) and an avidin: biotinylated enzyme complex (VECTASTAIN Elite ABC Reagent; Vector Laboratories, Inc., Burlingame, CA, USA) for FGF23 and ACE2, and a universal immunoperoxidase polymer (Histofine Simple Stain mouse MAX PO, anti-rat and anti-rabbit; Nichirei, Tokyo, Japan) for ACE and angiotensin II were used for immunostaining.

The percentage of positive areas of Sirius red staining, relative immune-positive area, and cardiomyocyte width and area in the LV sections were calculated as mean values in 20 randomly selected microscopic fields using ImageJ (ImageJ, U.S. National Institutes of Health, Bethesda, Maryland, USA). As for assessing the immune-positive area, the relative value was defined as that in each group or that in the sham group. All evaluations were performed in a blinded manner.

RNA Extraction And Real-time Polymerase Chain Reaction

As previously reported [12, 13], total RNA was extracted from the mouse heart and bone samples with an ISOGEN kit (Wako Pure Chemicals Industries, Ltd, Osaka, Japan) according to the manufacturer's instructions. ReverTra Ace™ qPCR RT Kit (TOYOBO Co., Ltd., Osaka, Japan) was used to create cDNA using an oligo-dT primer as recommended. The synthesized cDNA was stored at -80°C until analysis with quantitative PCR. mRNA expression was examined with real-time PCR using Applied Biosystems 7500 Real-Time PCR system (Thermo Fisher Scientific, Waltham, MA, USA) with the SYBR Green Assay with Thunderbird SYBR qPCR Mix (TOYOBO Co., Ltd., Osaka, Japan) following the manufacturer's protocol. The analysis was performed with the relative quantification method of the Applied Biosystems 7500 Real-Time PCR Software. The relative amount the mRNA samples was normalized to GAPDH mRNA. For PCR analysis, we used the following primers: α-myosin heavy chain (α-MHC), (5'-ATGTTAAGGCCAAGGTCGTG-3', 5'-CACCTGGTCCTCCTTTATGG-3'), β-myosin heavy chain (β-MHC), (5'-AGCATTCTCCTGCTGTTTCC-3', 5'-GAGCCTTGGATTCTCAAACG-3'), atrial natriuresis peptide (ANP), (5'-AGGCAGTCGATTCTGCTTGA-3', 5'-CGTGATAGATGAAGGCAGGAAG-3'), brain natriuresis peptide (BNP), (5'-TAGCCAGTCTCCAGAGCAATTC-3', 5'-TTGGTCCTTCAAGAGCTGTCTC-3'), collagen type I α2 (Col1a2), (5'-GCAGGTTCACCTACTCTGTCCT-3', 5'-CTTGCCCCATTCATTTGTCT-3'), collagen type III α1 (Col3a1), (5'-TCCCCTGGAATCTGTGAATC-3', 5'-TGAGTCGAATTGGGGAGAAT-3'), connective tissue growth factor (CTGF), (5'-CACAGAGTGGAGCGCCTGTTC-3', 5'-GATGCACTTTTTGCCCTTCTTAA-3'), FGF23, (5'-ACAAGGACACCTAAACCGAACAC-3', 5'-AGCTACTGACTGGTCCTATCACA-3'), AGT, (5'-TCTCTTTACCCCTGCCCTCT-3', 5'-GAAACCTCTCATCGTTCCTTG-3'), AT1R, (5
-ℂA ⊤ GTℂAℂ$CGATG$∀ G - 3′, 5′ - $TGCAGGTGAC$ ⊤ TGGℂAC - 3′), ACE, (5′ - ℂ$CTAGAG$∀ ∀ TCGℂ ⊤ C ⊤ G - 3′, 5′ - CG∀ $GATA$ℂAℂAGT
-TGGGCAAACTCTATGCTG-3', 5'-TTCATTGGCTCCGTTTCTTA-3'), Renin, (5'-CCTCTACCTTGCTTGTGGGATT-3', 5'-CTGGCTGAGGAAACCTTTGACT-3'), GAPDH, (3'-GCAAAGTGGAGATTGTTGCCA-5', 3'-AATTTGCCGTGAGTGGAGTCA-5').

Statistical analysis

Collected data were analyzed using the computer software application IBM SPSS statistics version 25.0 (IBM Corp., Armonk, NY, USA) for all statistical analyses. Values are presented as means ± SEM. The Mann–Whitney U test was used to analyze the significance of the differences between the two groups. The Kruskal-Wallis test was used to assess the differences between the four groups. Pearson's and Spearman's correlation coefficients were used to analyze relationships between the variables. A P value of < 0.05 was considered statistically significant.

Declarations

Conflict of interest statement

All authors declared no competing interests.

Author contributions

K.O. designed and performed experiments and wrote the manuscript. H.F., S.G., K.W., K.K., S.N. contributed to discussions. H.F. is the guarantor of this work and takes responsibility for the integrity of the data and the accuracy of the data analysis.

References

1. Gutierrez, O. et al. Fibroblast growth factor-23 mitigates hyperphosphatemia but accentuates calcitriol deficiency in chronic kidney disease. *J Am Soc Nephrol.* **16**, 2205–2215 (2005).
2. Blau, J. E. & Collins, M. T. The PTH-Vitamin D-FGF23 axis. *Rev Endocr metab Disord.* **16**, 165–174 (2015).
3. Orlando, M. et al. Fibroblast growth factor 23 and left ventricular hypertrophy in chronic kidney disease. *Circulation.* **119**, 2545–2552 (2009).
4. Faul, C. et al. FGF23 induces left ventricular hypertrophy. *J Clin Invest.* **121**, 4394–4408 (2011).
5. Slavic, S. et al. Genetic ablation of *Fgf23* or *Klotho* does not modulate experimental heart hypertrophy induced by pressure overload. *Sci Rep.* **7**, 11298; 10.1038/s41598-017-10140-4 (2017).
6. Takashi, Y. et al. Patients with FGF23-related hypophosphatemic rickets/osteomalacia do not present with left ventricular hypertrophy. *Endocr Res.* **42**, 132–137 (2017).

7. Mhatre, K. N. et al. Crosstalk between FGF23- and angiotensin II- mediated Ca^{2+} signaling in pathological cardiac hypertrophy. *Cell Mol Life Sci.* **75**, 4403–4416 (2018).
8. De Stefano, G. M. M. F. et al. Aldosterone is associated with left ventricular hypertrophy in hemodialysis patients. *Ther Adv Cardiovasc Dis.* **10**, 304–313 (2016).
9. Stein, A. B. et al. The PTIP-associated histone methyltransferase complex prevents stress-induced maladaptive cardiac remodeling. *Plos One.* **22**, e0127839; 10.1371/journal.pone.0127839. eCollection (2015)
10. Kilkenny, C., Browne, W. J., Cuthill, I.C., Emerson, M., Altman, D. G. Improving bioscience research reporting: The ARRIVE guidelines for reporting animal research. *PLoS Biol. **8***, e1000412 ; 10.1371/journal.pbio.1000412 (2010).
11. McGrath, J. C., Drummond, G. B., McLachlan, E. M., Kilkenny, C., Wainwright, C. L. Guideline for reporting experiments involving animals: the ARRIVE guidelines. *Br J Pharmacol.* **160**, 1573–1576 (2010).
12. Fujii, H. et al. Anti-oxidative effect of AST-120 on kidney injury after myocardial infarction. *Br J Pharmacol.* **173**, 1302-1313 (2016).
13. Fujii, H., Hamada, Y., Fukagawa, M. Bone Formation in Spontaneously Diabetic Torii - newly established model of non-obese Type 2 Diabetes rats. *Bone.* **42**, 372-379 (2008).
14. Lei, B. et al. Transient activation of p38 MAP kinase and up-regulation of Pim-1 kinase in cardiac hypertrophy despite no activation of AMPK. *J Mol Cell Cardiol.* **45**, 404–410 (2008).
15. Zhan, M. et al. Pathological cardiac hypertrophy alters intracellular targeting of phosphodiesterase type 5 from nitric oxide synthase-3 to natriuretic peptide signaling. *Circulation.* **126**, 942–951 (2012).
16. Rockman, H. A. et al. ANG II receptor blockade prevents ventricular hypertrophy and ANF gene expression with pressure overload in mice. *Am J Physiol.* **266**: H2468–2475 (1994).
17. Fujii, H. & Joki, N. Mineral metabolism and cardiovascular disease in CKD. *Clin Exp Nephrol.* **21**, 53–63 (2017).
18. Gutierrez, OM. *et al.* Fibroblast growth factor 23 and left ventricular hypertrophy in chronic kidney disease. *Circulation.* **119**, 2545–2552(2009).
19. Mirza, M. A. I., Larsson, A., Melhus, H., Lind, L., Larsson, T. E. Serum intact FGF23 associate with left ventricular mass, hypertrophy and geometry in an elderly population. *Atherosclerosis.* **207**, 546–551 (2009).
20. Grabner, A. et al. Activation of cardiac fibroblast growth factor receptor 4 causes left ventricular hypertrophy. *Cell Metab.* **22**, 1020–1032 (2015).
21. Matsui, I. et al. Cardiac hypertrophy elevates serum levels of fibroblast growth factor 23. *Kidney Int.* **94**, 60-71 (2018).
22. Fujii, H. et al. Changes in serum and intracardiac fibroblast growth factor 23 during the progression of left ventricular hypertrophy in hypertensive model rats. *Clin Exp Nephrol.* **23**, 589-596 (2019).
23. Mitsnefes, M. M. Betoko A, Schneider MF, et al. FGF23 and left ventricular hypertrophy in children with CKD. *Clin J Am Soc Nephrol.* **13**, 45-52 (2018).
24. Böckmann, I. et al. FGF23-mediated activation of local RAAS promotes cardiac hypertrophy and fibrosis. *Int J Mol Sci.* **20**, 4634; 10.3390/ijms20184634 (2019).
25. Pi, M. et al. Cardiovascular interactions between fibroblast growth factor-23 and angiotensin II. *Sci Rep.* **8**, 12398; 10.1038/s41598-018-30098-1 (2018).
26. Zhang, B. et al. Up-regulation of FGF23 release by aldosterone. *Biochem Biophys Res Commun.* **470**, 384–390 (2016).
27. Nestler, M. L. et al. Fibroblast growth factor 23 is induced by an activated renin-angiotensin-aldosterone system in cardiac myocytes and promotes the pro-fibrotic crosstalk between cardiac myocytes and fibroblasts. *Nephrol Dial Transplant.* **18**, 33: 1722–1734 (2018).
28. Shimada, T. et al. FGF-23 is a potent regulator of vitamin D metabolism and phosphate homeostasis. *J Bone Miner Res.* **19**, 429–435 (2004).
29. Li, Y. C. et al. 1, 25-Dihydroxyvitamin D_3 is a negative endocrine regulator of the renin-angiotensin system. *J Clin Invest.* **110**, 229–238 (2002).
30. Chen, S. et al. Cardiomyocyte-specific deletion of the vitamin D receptor gene results in cardiac hypertrophy. *Circulation.* **124**, 1838–1847 (2011).
31. Fujii, H. et al. The Vitamin D receptor activator maxacalcitol provides cardioprotective effects in diabetes mellitus. *Cardiovasc Drugs Ther.* **29**, 499–507 (2015).
32. Santos, R. A., Ferreira, A. J., Verano-Braga, T., & Bader, M. et al. Angiotensin converting enzyme 2, angiotensin-(1-7) and Mas: new players of the renin-angiotensin system. *J Endocrinol.* **216**, R1-R17 (2013).
33. Burns, K. D. The emerging role of angiotensin-converting enzyme-2 in the kidney. *Curr Opin Nephrol Hypertens.* **16**, 116-121 (2007).
34. Crackower, M. A. et al. Angiotensin-converting enzyme 2 is an essential regulator of heart function. *Nature.* **417**, 822–828 (2002).
35. Bodiga, S. et al. Enhanced susceptibility to biomechanical stress in ACE2 null mice is prevented by loss of the p47 (phox) NADPH oxidase subunit. *Cardiovasc Res.* **91**, 151–161 (2011).
36. Oudit, G. Y. et al. Angiotensin II-mediated oxidative stress and inflammation mediate the age-dependent cardiomyopathy in ACE2 null mice. *Cardiovasc Res.* **75**, 29–39 (2007).
37. Dai, B. et al. A comparative transcriptome analysis identifying FGF23 regulated genes in the kidney of a mouse CKD model. *PLoS One.* 7, e 44161; 10.1371/journal.pone.0044161 (2012).
38. Anguiano, L. et al. Circulating angiotensin-converting enzyme 2 activity in patients with chronic kidney disease without previous history of cardiovascular disease. *Nephrol Dial Transplant.* **30**, 1176–1185 (2015).
39. Lang, F. et al. Phosphate Homeostasis, Inflammation and the Regulation of FGF-23. *Kidney Blood Press Res.* **43**, 1742–1748 (2018).

Tables

Table 1. Animal characteristics at 16 weeks

	Sham (N = 6)	CKD (N = 6)	LVH (N = 6)	CKD/LVH (N = 6)
Body weight (g)	29. 5± 0.7	25.1 ± 0.8$^{\#}$	28.7 ± 0.6*	25.7 ± 1.0$^{\#,▯}$
SBP (mmHg)	86.2 ± 0.6	97.6 ± 2.0$^{\#}$	87.2 ± 1.8	107.2 ± 4.0$^{\#,▯}$
HR (/min)	516.3 ± 12.3	493.1 ± 12.2	490.7 ± 15.4	472.8 ± 14.7
Cr (mg/dL)	0.14 ± 0.02	0.44 ± 0.03$^{\#}$	0.23 ± 0.02*	0.47 ± 0.09$^{\#,▯}$
Ca(mg/dL)	9.87 ± 0.30	9.83 ± 0.80	10.03 ± 0.76	9.02 ± 0.81
P (mg/dL)	8.1 ± 0.6	9.7 ± 0.4$^{\#}$	8.8 ± 0.3	10.3 ± 0.3$^{\#}$
iPTH (pg/mL)	29.0 ± 11.6	77.6 ± 16.2	50.6 ± 7.0	111.6 ± 39.1$^{\#}$
25(OH)D (pg/mL)	61.7 ± 2.3	61.8 ± 3.5	59.7 ± 3.2	63.3 ± 4.0
1, 25$(OH)_2$D (pg/mL)	227.0 ± 18.9	184.8 ± 10.4	222.2 ± 24.6	178.0 ± 9.9
uAGT (ng/mgCr)	3.32 ± 0.85	3.36 ± 0.94	7.13 ± 2.55$^{\#,*}$	9.62 ± 2.10$^{\#,*}$
uAlb (μg/mgCr)	144.6 ± 9.5	1156.3 ± 221.2$^{\#}$	156.1 ± 5.7*	1356.8 ± 145.6$^{\#,▯}$
u8-OHdG (ng/mgCr)	53.9 ± 1.8	99.4 ± 16.1$^{\#}$	82.8 ± 8.3	101.3 ± 9.2$^{\#}$

$^{\#}$: vs Sham, $P < 0.05$, *: vs CKD, $P < 0.05$, ▯: vs LVH, $P < 0.05$.
CKD, chronic kidney disease; LVH, left ventricular hypertrophy; SBP, systolic blood pressure; HR, heart rate; Cr, creatinine; Ca, calcium; P, phosphate; iPTH, intact parathyroid hormone; uAGT, urinary angiotensinogen; uAlb, urinary albumin; u8-OHdG, urinary 8-hydroxy-2'-deoxyguanosine.

Table 2. Animal characteristics at 16 weeks

Sham (N = 6)	CKD (N = 6)	LVH (N = 6)	CKD/LVH (N = 6)	
LVDd (mm)	3.77 ± 0.76	3.45 ± 0.76	3.47 ± 0.29	3.15 ± 0.08
LVDs (mm)	2.78 ± 0.06	2.67 ± 0.06	2.75 ± 0.22	2.55 ± 0.07$^{\#,*}$
LVAW (mm)	0.75 ± 0.02	0.80 ± 0.04	1.23 ± 0.04$^{\#,*}$	1.30 ± 0.04$^{\#,*}$
LVPW (mm)	0.71 ± 0.03	0.75 ± 0.04	1.18 ± 0.05$^{\#,*}$	1.20 ± 0.04$^{\#,*}$
FS (%)	25.8 ± 0.4	23.0 ± 0.2$^{\#}$	20.9 ± 0.3$^{\#,*}$	19.3 ± 0.8$^{\#,*}$
EF (%)	57.7 ± 0.6	52.9 ± 0.4	49.1 ± 0.5$^{\#,*}$	46.0 ± 1.7$^{\#,*}$
Heart weight (mg)	131.3 ± 3.3	116.2 ± 2.3	181.6 ± 5.2$^{\#,*}$	178.2 ± 8.5$^{\#,*}$
Relative heart weight (mg/g)	4.45 ± 0.07	4.64 ± 0.08	6.33 ± 0.16$^{\#,*}$	6.96 ± 0.36$^{\#,*}$

$^{\#}$: vs Sham, $P < 0.05$, *: vs CKD, $P < 0.05$, ▯: vs LVH, $P < 0.05$.
CKD, chronic kidney disease; LVH, left ventricular hypertrophy; LVDd, left ventricular diastolic diameter; LVDs, left ventricular systolic diameter; LVAW, left ventricular anterior wall; LVPW, left ventricular posterior wall; FS, fractional shortening; EF, ejection fraction.

Table 3. Correlation of each FGF23 and RAAS data with cardiac parameters

	HW	rHW	Width	Area	Fibrosis	LVAW	LVPW	FS	EF	cANP	cBNP	cα-MHC	cβ-MHC	cCol1a2	cCol3a1
3	.212	.517**	.617**	.518**	.698**	.449*	.394	-.639**	-.645**	.329	.299	-.181	.583**	.493*	.528**
3	.536**	.708**	.641**	.717**	.807**	.726**	.707**	-.816**	-.805**	.399	.436*	-.512*	.846**	.709**	.445*
23	.505*	.766**	.649**	.815**	.890**	.728**	.709**	-.820**	-.814**	.403	.538**	-.569**	.838**	.683**	.487*
	.251	.641**	.666**	.495*	.616**	.564**	.566**	-.629**	-.625**	.241	.239	-.241	.527**	.500*	.423*
2	.624**	.765**	.679**	.830**	.768**	.702**	.644**	-.858**	-.863**	.369	.427*	-.651**	.742**	.555**	.443*
	.537**	.674**	.730**	.678**	.662**	.779**	.700**	-.692**	-.691**	.490*	.352	-.703**	.742**	.497*	.473*
	.823**	.784**	.600**	.683**	.628**	.735**	.705**	-.717**	-.714**	.441*	.448*	-.773**	.738**	.457*	.335
2	-.690**	-.778**	-.613**	-.701**	-.622**	-.752**	-.702**	.714**	.704**	-.528**	-.311	.803**	-.699**	-.400	-.226
	.485*	.572**	.528**	.557**	.557**	.744**	.694**	-.624**	-.612**	.116	.213	-.539**	.683**	.510*	.312
II	.448*	.656**	.651**	.562**	.637**	.665**	.613**	-.672**	-.676**	.301	.283	-.561**	.714**	.389	.277
2	.700**	.836**	.779**	.853**	.824**	.837**	.821**	-.884**	-.881**	.462*	.561**	-.695**	.834**	.645**	.444*
2	-.690**	-.776**	-.664**	-.586**	-.643**	-.834**	-.794**	.706**	.705**	-.489*	-.476*	.719**	-.786**	-.437*	-.423*

*: $P < 0.05$, **: $P < 0.01$.
HF, heart weight; rHF, relative heart weight; LVAW, left ventricular anterior wall; LVPW, left ventricular posterior wall; FS, fractional shortening; EF, ejection fraction; cANP, cardiac atrial natriuresis peptide; cBNP, cardiac brain natriuresis peptide; cα-MHC, cardiac α-myosin heavy chain; cCol1a2, cardiac collagen type I α2; cCol3a1, cardiac collagen type III α1; iFGF23, intact

fibroblast growth factor 23; cFGF23, cardiac fibroblast growth factor 23; imFGF23, immunohistochemical expression of cardiac fibroblast growth factor 23; Ald, aldosterone; cAT1R, cardiac angiotensin II type 1 receptor; cAGT, cardiac angiotensinogen; cACE, cardiac angiotensin-converting enzyme; cACE2, cardiac angiotensin-converting enzyme 2; uAGT, urinary angiotensinogen; imAng II, immunohistochemical expression of cardiac angiotensin II; imACE, immunohistochemical expression of cardiac angiotensin-converting enzyme; imACE2, immunohistochemical expression of cardiac angiotensin-converting enzyme 2.

Table 4. Correlation of each FGF23 data with RAAS-related factors

	Ald	cAT1R	cAGT	cACE	cACE2	uAGT	imAng II	imACE	imACE2
iFGF23	.388	.665**	.556**	.285	-.269	.164	.511*	.518**	-.297
cFGF23	.567**	.780**	.722**	.663**	-.689**	.626**	.713**	.785**	-.666**
imFGF23	.554**	.820**	.762**	.664**	-.623**	.554**	.729**	.862**	-.705**

Ald, aldosterone; cAT1R, cardiac angiotensin II type 1 receptor; cAGT, cardiac angiotensinogen; cACE, cardiac angiotensin-converting enzyme; cACE2, cardiac angiotensin-converting enzyme 2; uAGT, urinary angiotensinogen; imAng II, immunohistochemical expression of cardiac angiotensin II; imACE, immunohistochemical expression of cardiac angiotensin-converting enzyme; imACE2, immunohistochemical expression of cardiac angiotensin-converting enzyme 2; iFGF23, intact fibroblast growth factor 23; cFGF23, cardiac fibroblast growth factor 23; imFGF23, immunohistochemical expression of cardiac fibroblast growth factor 23.

Figures

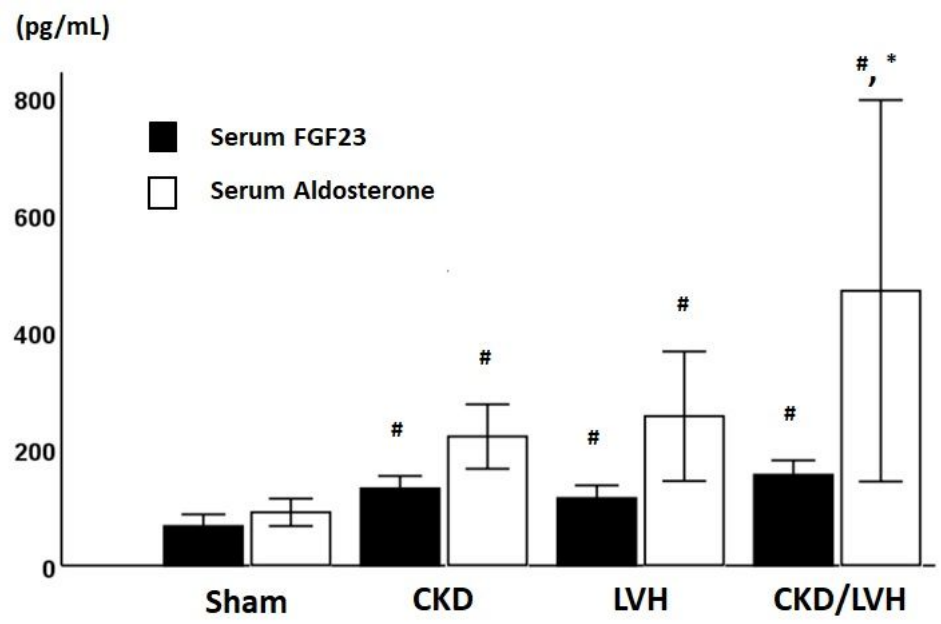

Figure 1

Serum FGF23 and aldosterone levels among the study groups. Black bar: serum FGF23 levels White bar: serum aldosterone levels #: vs Sham group, P<0.05; *: vs CKD group, P<0.05.

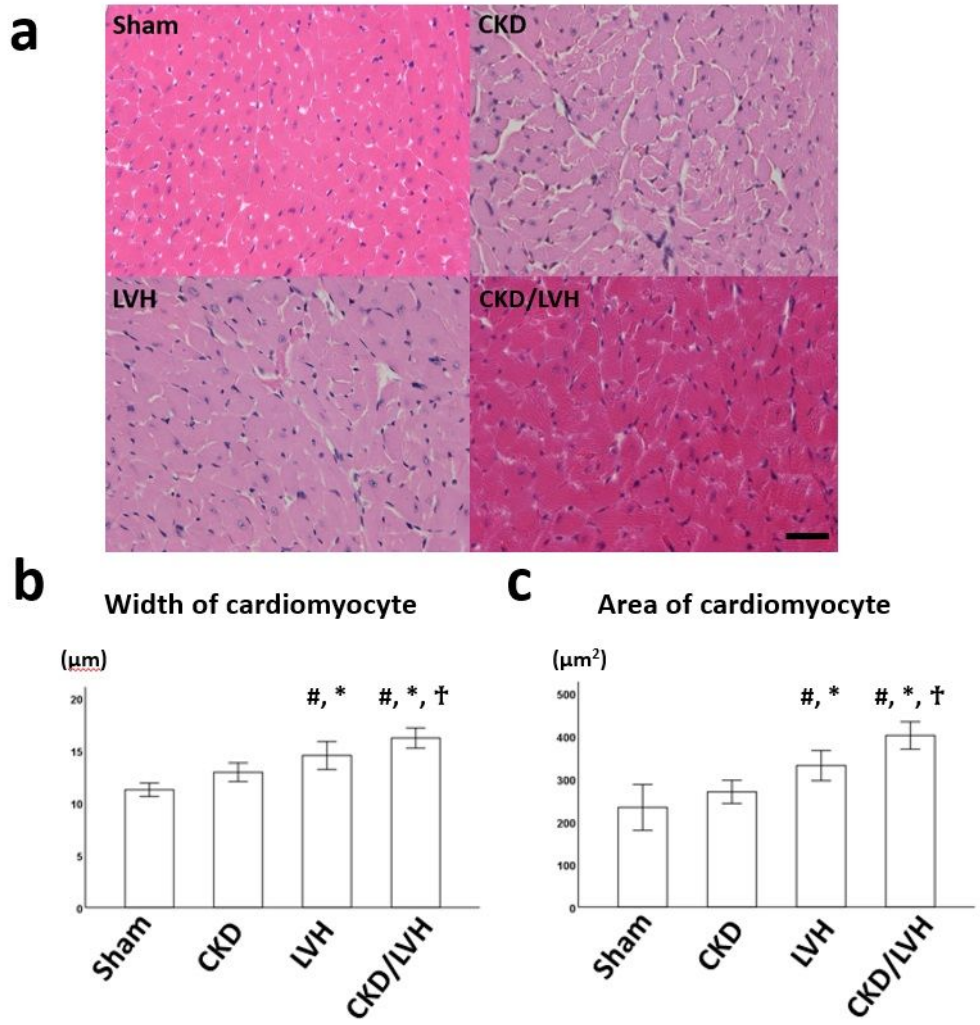

Figure 2

Histological measurement of cardiomyocytes. Representative photomicrographs of cardiomyocytes with hematoxylin-eosin (magnification, ×400; Bar = 20 μm) Left upper panel, sham group; right upper panel, CKD group; left lower panel, LVH group; right lower panel, CKD/LVH group (CKD, chronic kidney disease; LVH, left ventricular hypertrophy). a. Width of cardiomyocytes b. Area of cardiomyocytes Values are expressed as means ± SEM. #: vs Sham, $P < 0.05$; *: vs CKD, $P < 0.05$; †: vs LVH, $P < 0.05$.

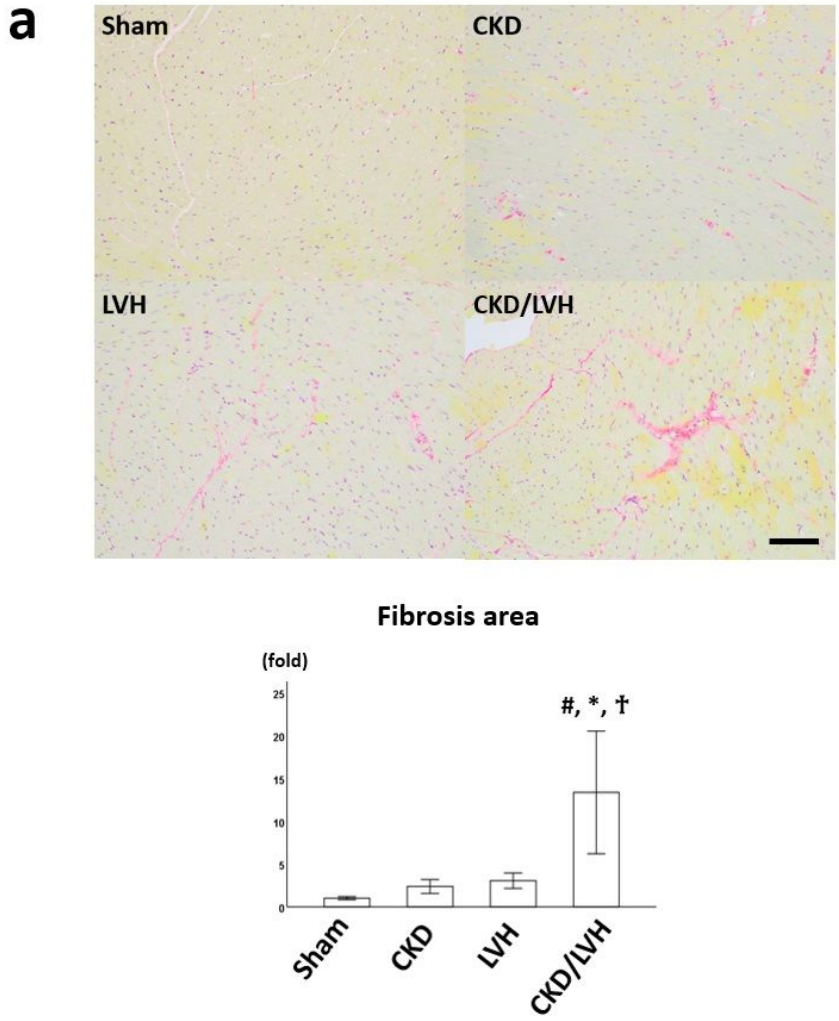

Figure 3

Evaluation of cardiac fibrosis. a. Representative photomicrographs of cardiomyocytes with Sirius red (magnification, ×400; Bar = 20 μm) Left upper panel, sham group; right upper panel, CKD group; left lower panel, LVH group; right lower panel, CKD/LVH group (CKD, chronic kidney disease; LVH, left ventricular hypertrophy). b. Fibrosis area of the heart Values are expressed as means ± SEM. #: vs Sham, P < 0.05; *: vs CKD, P < 0.05; †: vs LVH, P < 0.05.

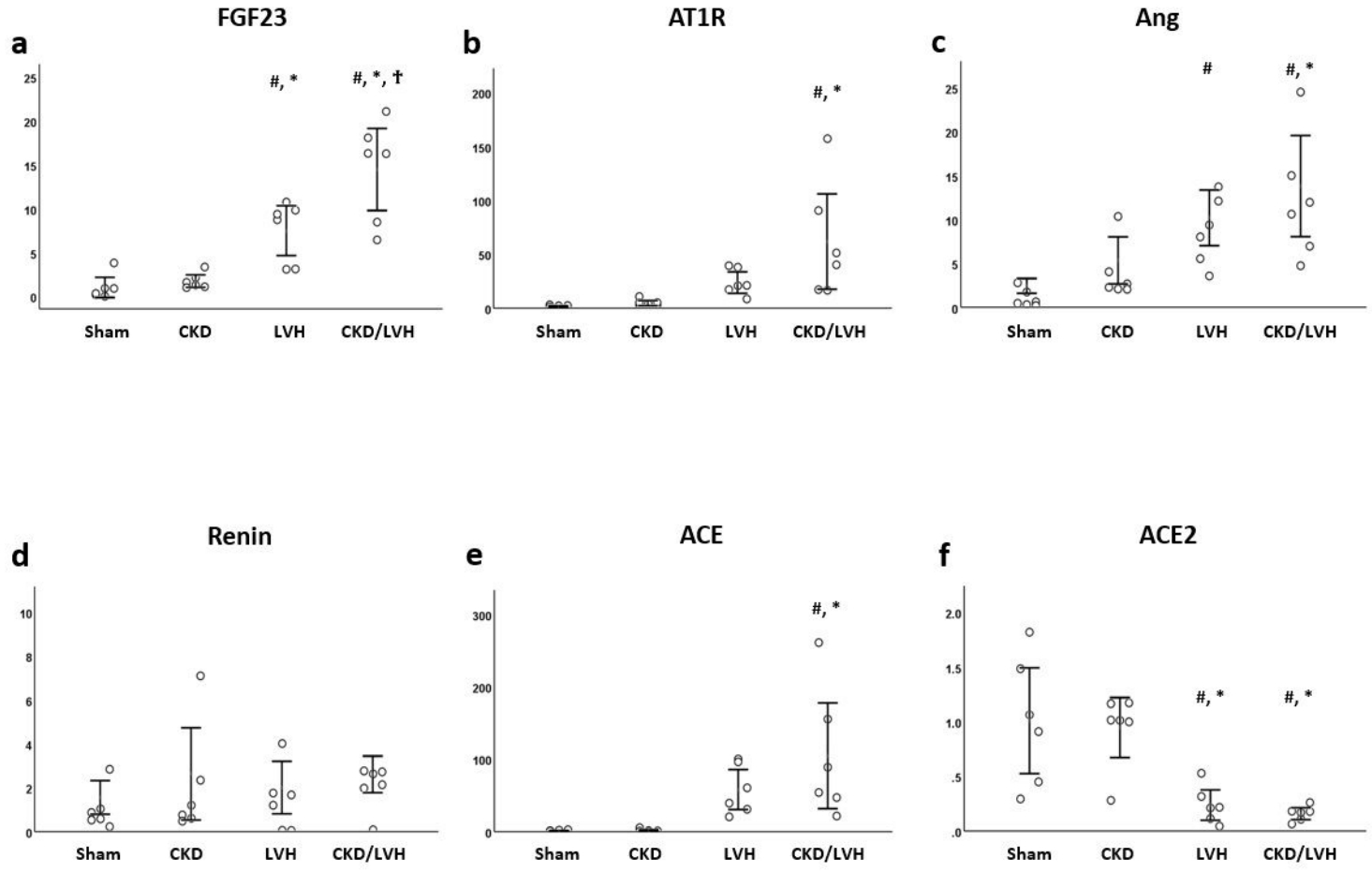

Figure 4

mRNA expressions of FGF23 and RAAS-related factors in the heart. a. Fibroblast growth factor 23 (FGF23) b. Angiotensin II type 1 receptor (AT1R) c. Angiotensinogen (Ang) d. Renin e. Angiotensin-converting enzyme (ACE) f. Angiotensin-converting enzyme 2 (ACE2) Values are expressed as means ± SEM. #: vs Sham, P < 0.05; *: vs CKD, P < 0.05; †: vs LVH, P < 0.05.

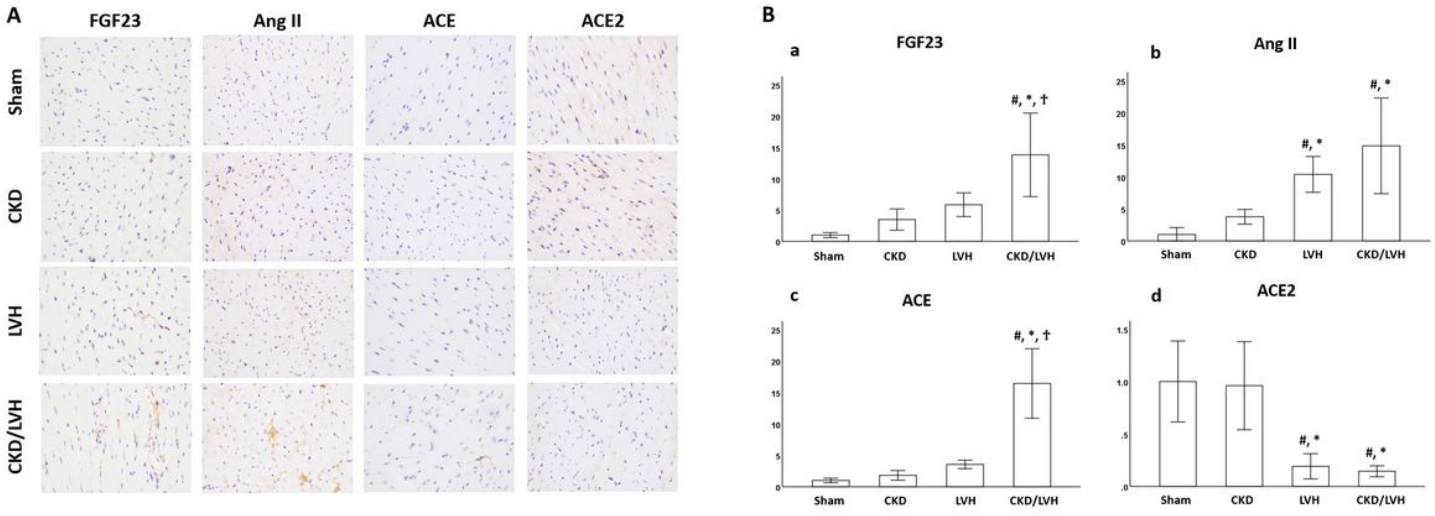

Figure 5

Evaluation of the expressions of FGF23 and RAAS-related factors by immunohistochemical staining. A. Representative photomicrographs of cardiomyocytes with immunohistochemical staining for FGF23 and each RAAS-related factors B. Semiquantitative evaluation of FGF23 and each RAAS-related factors in the heart a. Fibroblast growth factor 23 (FGF23) b. Angiotensin II (Ang II) c. Angiotensin-converting enzyme (ACE) d. Angiotensin-converting enzyme 2 (ACE2) Values are expressed as means ± SEM. #: vs Sham, P < 0.05; *: vs CKD, P < 0.05; †: vs LVH, P < 0.05.

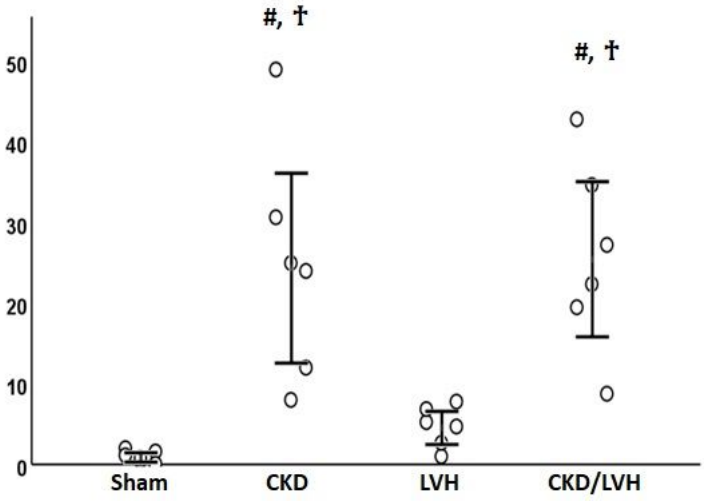

Figure 6

mRNA expression of FGF23 in bone. Values are expressed as means ± SEM. #: vs Sham, P < 0.05; †: vs LVH, P < 0.05.

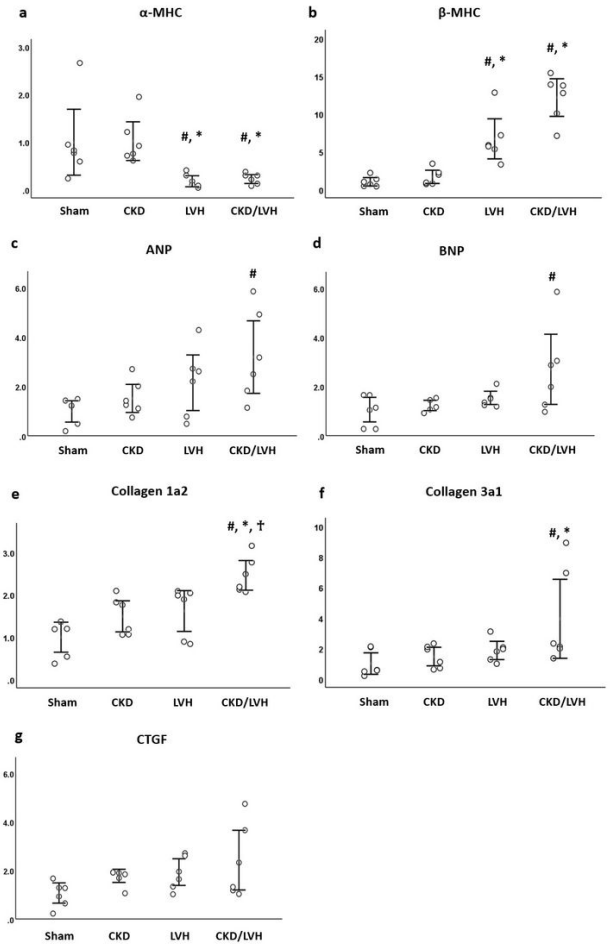

Figure 7

mRNA expressions of cardiac hypertrophy and fibrosis-related factors in heart. a. α-myosin heavy chain (α-MHC) b. β-myosin heavy chain (β-MHC) c. collagen type I α2 (Collagen 1a2) d. collagen type III α1 (Collagen 3a1) Values are expressed as means ± SEM. #: vs Sham, $P < 0.05$; *: vs CKD, $P < 0.05$; : vs LVH, $P < 0.05$.